Catalysis Today 177 (2011) 79–86

Contents lists available at ScienceDirect

Catalysis Today

journal homepage: www.elsevier.com/locate/cattod

Competitive ligand/chelate binding in [Cu(TMPA)]$^+$ and [Cu(tren)]$^+$ based complexes

Lauréline Bonniard[a,b], Aurélien de la Lande[a,b,c], Simon Ulmer[a,b], Jean-Philip Piquemal[a,b], Olivier Parisel[a,b], Hélène Gérard[a,b,*]

[a] UPMC Univ Paris 06, UMR 7616, Laboratoire de Chimie Théorique, case courrier 137, 4 place Jussieu, F. 75005 Paris, France
[b] CNRS, UMR 7616, Laboratoire de Chimie Théorique, case courrier 137, 4 place Jussieu, F. 75005 Paris, France
[c] Laboratoire de Chimie Physique – CNRS UMR 8000, Université Paris-Sud 11, Bât. 349, Campus d'Orsay, 15, rue Jean Perrin, 91405 Orsay Cedex, France

ARTICLE INFO

Article history:
Received 1 May 2011
Received in revised form 12 July 2011
Accepted 14 July 2011
Available online 24 August 2011

Keywords:
N3N ligands
Copper(I) complexes
Dioxygen
Alcohol oxidation

ABSTRACT

The competition between coordination of an incoming ligand (CO, CH_3CN, PH_3, H_2O, MeOH, PhOH and O_2 in its triplet state) and decoordination of one arm of the tripod is examined in the case of the [Cu(TMPA)]$^+$ and [Cu(tren)]$^+$ complexes from a theoretical point of view. It is shown that in the case of strong ligand (CO, CH_3CN and PH_3), arm and ligand coordination are competitive but that coordination of both is the most favored structure. In the case of ROH ligands, a structure with one arm decoordinated and interacting through H-bond with the hydroxyl hydrogen is found. This structure is of special interest as it allows liberation of one bonding site, which can be used for further dioxygen coordination. The consequences of these results on the oxidation of alcohols by dioxygen catalyzed by these classes of complexes are discussed.

1. Introduction

In the course of the development of innovative concepts and synthetic tools toward greener chemical processes [1,2], the use of O_2 as an oxidant has drawn sustained attention in the last decade. As an illustration of the chemical procedures involving O_2 as the primary oxidative species, the so-called *biomimetic* approach has been inspired from the way dioxygen is activated in living systems [3]. In various metalloenzymes, dioxygen activation is effectively supported by copper (I) or copper (II) active sites that can in turn be modeled by copper complexes built on polydentate N-donating ligands [4,5]. Such species were shown to catalyze four electron reduction of dioxygen [6]. Among them, two classes of neutral N_3N ligands (Scheme 1) such as tris(2-methylpyridyl)amine or tris(2-aminoethyl)amine (thereafter respectively referred to as TMPA and tren, respectively) have drawn our attention [7–14] due both to their incorporation in a large variety of structures [15–18] and to their remarkable versatility from the view point of both coordination mode [19] and reactivity [4] toward dioxygen. Among other properties, [Cu(TMPA^R)]$^+$ and [Cu(tren$^{R,R'}$)]$^+$ complexes can form either a 1:1 or a 2:1 copper-dioxygen adducts upon addition of dioxygen [4,19]. As a consequence, depending on the experimental conditions and the exact substitution at the TMPA^R or tren$^{R,R'}$ moieties (Scheme 1), they can thus be considered as bio-inspired models of enzymes containing either a CuO_2 or a Cu_2O_2 core. Regarding the reactivity of the copper-dioxygen adduct toward exogenous substrates, numerous examples of reactivity of the 2:1 compounds have been reported, while fewer is known about the oxidative capabilities of 1:1 adducts toward organic substrates [4]. Recent investigations suggesting that oxidative reactions can take place using 1:1 adducts such as [Cu(TMPA^{NMe2})(O_2)]$^+$ [20] or [Cu(tren^{TMG,TMG})(O_2)]$^+$ [21] drew our attention (Scheme 1) as they point out the potential sensitivity of this reactivity to the exact nature of the R and R′ substituent.

Understanding the molecular grounds of copper-dioxygen catalysis is challenging and has actually stimulated numerous theoretical studies dealing mostly with structural, energetic or electronic aspects of the oxidation mechanisms. Dioxygen coordination modes and energies have been examined and compared to experimental data. The subsequent reactivity toward an exogeneous substrate has then often been considered as an intermolecular mechanism [22] which is surprising as a common role of metal complexes in catalyzing multimolecular reactions relies on their capabilities of coordinating all reactive species onto a single metal center, gathering them in a reaction-adapted geometry to avoid entropically costly rearrangements. In the case of these

* Corresponding author at: UPMC Univ Paris 06, UMR 7616, Laboratoire de Chimie Théorique, case courrier 137, 4 place Jussieu, F. 75005 Paris, France.
Tel.: +33 1 44 27 96 62; fax: +33 1 44 27 41 17.
E-mail address: helene.gerard@upmc.fr (H. Gérard).

0920-5861/$ – see front matter © 2011 Elsevier B.V. All rights reserved.
doi:10.1016/j.cattod.2011.07.015

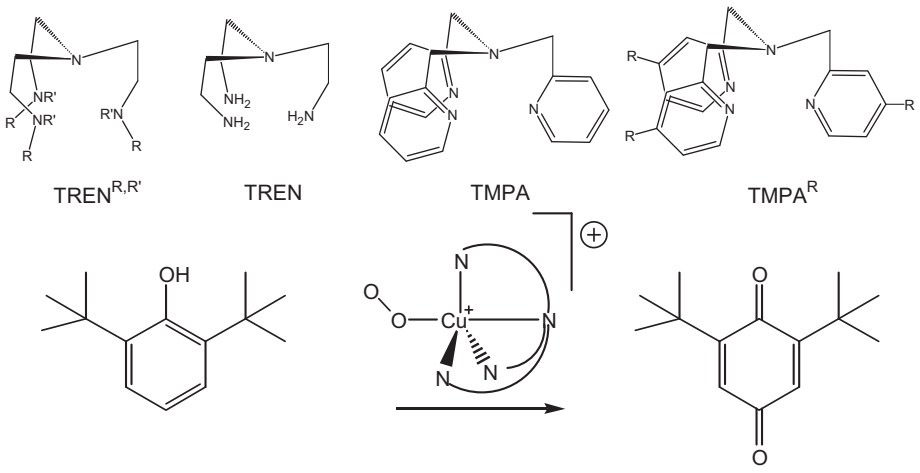

Scheme 1.

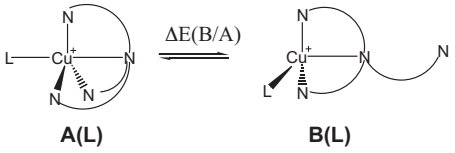

Scheme 2.

N_3N ligands, the simultaneous coordination of O_2 and of the reactive substrate requires the liberation of a coordination site, as only one vacancy is available in the initial $[Cu(N_3N)]^+$ complex. This can be obtained *via* decoordination of one of the arm of the ligand (Scheme 2), a process for which evidences have been reported in the literature for some $TMPA^R$ complexes, either on XRay structures [23], NMR data [24] or formed under photochemical activation [25] but, to our knowledge, not for the $tren^{R,R'}$ ones.

The objective of the present contribution is thus to investigate this possibility in the case of the prototype $TMPA^H$ and $tren^{H,H}$ complexes, and to examine the possible mechanistic consequences on the reactive properties of the copper-dioxygen adducts. The prototype ligands L = CO [25], CH_3CN [24] and PH_3 [23] will be first examined within the framework of the structural and energetic description of the decoordination described in Scheme 2. This is especially significant as evidences for such decoordination of one arm have been reported for all three ligands in systems closely related to $[Cu(TMPA)]^+$. We will next turn to the biologically relevant water and alcohol ligands, the latest being the substrate of the oxidation processes observed experimentally (Scheme 1). Finally, the coordination of O_2 in the absence or in the presence of alcohol or water is examined and various conclusions related to the catalytic reactivity within these species will be drawn.

2. Computational details

Full geometry optimizations were conducted without symmetry restraints using the Gaussian 03 program. [26] The DZVP2 basis set was employed for all atoms. [27] A set of p diffuse functions was added on oxygen and nitrogen. [28,29] For the Density Functional Theory (DFT) calculations, the hybrid B3LYP exchange-correlation functional [30–33] was used in its unrestricted formalism when triplet states are considered. The B3LYP functional has proven to successfully predict correct association energies of ligands to Cu(I) [34,35]. All results are given without BSSE correction, as this one is not expected to modify the general trends examined here [9]. The quality of the obtained electronic properties is confirmed on $[Cu(TMPA)^R(CO)]^+$ complexes (R = H or NH_2) by comparison of the computed ν_{CO} vibrational frequencies scaled by a factor of 0.97 [36] to experimental data (Table 1). The computed values are within 3 cm^{-1} of the experimental ones and the variations upon changing group R within 1 cm^{-1} of the experimental values.

In our study, we report various energetic data:

$E(X)$ is the energy of structure X with respect to the reference. The common reference used throughout this work is the $[Cu(N_3N)]^+$ complex in absence of L ligand, further referred to as **A(Ø)**. $E(X)$ is thus computed as the energy for the optimized **X(L)** structure with respect to the optimized non-coordinated complex **A(Ø)** and the optimized ligand **L**.

$\Delta E(X/Y)$ is the relative energy of structure X with respect to structure Y, structures X and Y having the same chemical composition. In particular, $\Delta E(B/A)$ is the energy of complex **B(L)** with respect to complex **A(L)** and thus corresponds to decoordination of one of the tripod arm. $\Delta E(X/Y)$ is computed as the energy difference between the optimized **X(L)** complex and the optimized **Y(L)** complex.

$\Delta E_c(X)$ is the coordination energy of ligand **L** in structure **X(L)** and is taken as the energy difference between optimized structure for **X(L)** and the sum of the energies of optimized non-coordinated complex **X(Ø)** and optimized ligand **L**. Let us notice that $\Delta E_c(A) = E(A)$.

Binding energies were checked for a potential influence of basis set superposition error (BSSE) on selected structures: the prototype ligand CO was examined, together with O_2 and H_2O (considered as a model of alcohol). The BSSE were computed using the counterpoise method as implemented in the Gaussian program [37,38]. Its value for the L binding energy within the **A(L)** structures varies between 2.1 kcal mol^{-1} for the weakly bonded H_2O ligand and 6.6 kcal mol^{-1} for the more strongly bonded CO. In contrast, the influence of BSSE on reaction energy is found to be small. For instance, it is always less than 1 kcal mol^{-1} for the **A(L)** → **B(L)** process. For selected structures, importance of adding an implicit solvation was examined using single point computations on gas phase optimized geometry. These results are reported in Table 2. For these computations,

Table 1
Computed CO vibrational frequencies as a function of TMPA functionalization compared to experimental data.

	ν_{exp} (cm^{-1})	$\nu_{computed}$ (cm^{-1})	
		Unscaled	Scaled
$[(CO)Cu(TMPA)]^+$	2092	2153	2089
$[(CO)Cu(TMPA^{pNMe2})]^+$	2079	2141	2077

Table 2
Corrections to the energies due to solvation by a continuum model (correction to the energy for processes $X \rightarrow Y$ described in column two, in kcal mol^{-1}).

	Solvation using a continuum		
	Process	$\Delta(\Delta E_{Y/X})$ for TMPA	$\Delta(\Delta E_{Y/X})$ for TREN
L = CO	A → B	1.02	0.63
L = O_2	A → B	0.04	−0.79
L = H_2O	A → C	1.30	NC

the PCM model with the dielectric constant implemented for THF (ε_R = 7.58) [39] and the default implemented in Gaussian 03 is used, except for acidic hydrogen for which an additional sphere is added. The effects are found to be small and not sufficient to reverse the general trends discussed in this article. The results presented in the following study thus do not account for implicit solvation. In addition, as the solvent used experimentally is not a H-bond donor, no explicit inclusion of solvent was carried out.

Similar values can be estimated for Gibbs free energies and are respectively labeled as $G(X)$, $\Delta G(X/Y)$ and $\Delta G_c(X)$. To this end, the vibrational frequencies were computed within the harmonic approximation and used without scaling procedure; and the estimation of the thermal and entropic corrections have been obtained on the basis of statistic thermodynamics approximation at T = 213 K which is a common experimental temperature [20,21]. The nature of the transition states was ensured by confirming the presence of a single imaginary frequency. The connection between transition states and minima were ensured by carrying out small displacements of all atoms in the two directions along the imaginary frequency mode and carrying out geometry optimization using these geometries as starting points. Partial atomic charges (NPA) have been evaluated according to the Natural Bonding Orbital (NBO) approach [40].

3. Prototype ligands: L = CO, CH_3CN and PH_3

The structures of the **A(CO)** and **A(CH_3CN)** complexes built on the tren ligand have already been examined in previous studies devoted to the [Cu(tren)(L)]$^+$ complexes [9] and were found similar to those obtained for the [Cu(TMPA)(L)]$^+$ complexes. The following geometrical descriptors are used to quantify the deviations from a perfect trigonal pyramid geometry (bipyramid geometry in presence of fifth ligand L) (Fig. 1 and Table 3)

(i) The basal dihedral angle $\Omega = N_{bas}–Cu–N_{bas}–N_{bas}$, is close to 180° (153° for TMPA and 160° for tren) in the absence of ligand L, namely for **A(Ø)** complexes. Significant out-of-plane distortions take place upon coordination of L, and Ω decreases between 123° and 128° for structures **A(L)** (L = CO, CH_3CN and PH_3), with little effect with respect to the nature of L or to the N_3N tripod.
(ii) Another structural indicator is the average $N_{ap}–Cu–N_{bas}$ angle, referred to as Σ. Values of Σ are quasi-identical for the tren and the TMPA derived complexes with deviation less than 2° in all four structures reported in Table 3. Binding of the fifth ligand L significantly decreases Σ from about 83° to about 72°, without any significant effect with respect to the nature of the N_3N tripod or to that of the nature of ligand L.
(iii) In all cases, exogenous ligand L is perfectly coordinated in *trans* position with respect to the apical ligand as testified by the $N_{ap}–Cu–L$ angle which are all found to be very close to 180°.

In contrast to the angular properties described above, the Cu–N distances are sensitive to the chemical nature of both the tripod and ligand L, in a manner that can be easily rationalized on the basis of the nature of the nitrogen binding centers and of the flexibility of the tripod:

(i) Since the apical nitrogen is a tertiary amine nitrogen for tren and TMPA, the $Cu–N_{ap}$ bond lengths are identical in the absence of exogenous ligand L (structure **A(Ø)**) whereas the $Cu–N_{bas}$ bond lengths are found to be shorter when bonding is ensured by the sp^2 nitrogen lone pair of the TMPA (2.04 Å) than when ensured by the (higher in energy and thus less σ donating) sp^3 lone pair of the tren (2.11 Å).
(ii) Upon binding of exogenous ligand L (structure **A(L)**), the $Cu–N_{bas}$ bond lengths slightly increase, by 0.09 Å up to 0.15 Å, depending on the nature of the N_3N moiety and of ligand L. A much larger lengthening is observed for the $Cu–N_{ap}$ distance which increases from about +0.25 Å for TMPA to about +0.45 Å for tren. This is consistent with a more flexible structure of the tren ligand, which allows a more complete decoordination of the apical ligand upon coordination of L.

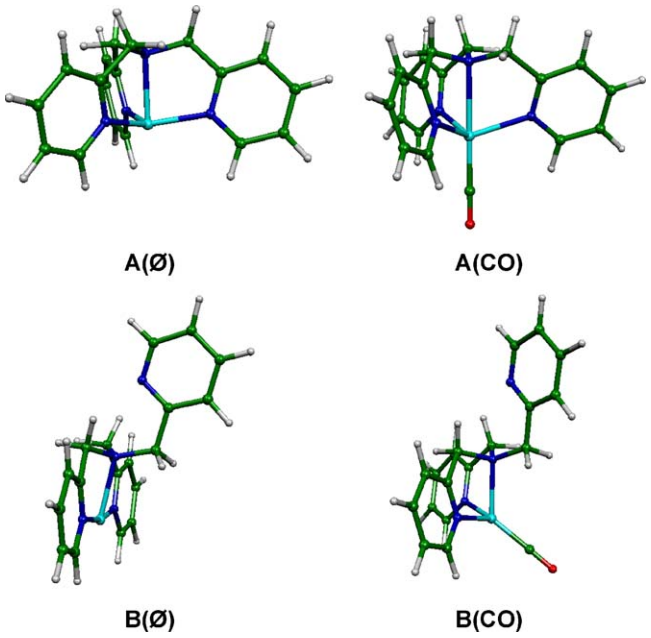

Fig. 1. Representations of structures A and B in the absence of ligand (left, top **A(Ø)** and bottom **B(Ø)**) or in the presence of CO (right, top A(CO) and bottom B(CO)).

We next turn to the decoordination of one of the arms of the N_3N tripod. These structures were optimized in the absence of ligand (**B(Ø)** structure) and then for L = CO, CH_3CN and PH_3 (**B(L)** structures). In all cases, the decoordination of one arm leads to additional major reorganizations of the binding at copper, in a similar way for both the tren and the TMPA complexes:

(i) In the absence of ligand, the trigonal pyramid structure of **A(Ø)** turns to a T-shaped coordination in **B(Ø)**, as illustrated on Fig. 1 and by the increase of the $N_{bas}–Cu–N_{bas}$ angles which come close to 180° in **B(Ø)**. This increase is larger for TMPA (168°) than for tren (158°) and is associated to a lengthening of the $Cu–N_{ap}$ distance and a shortening of the $Cu–N_{bas}$ ones.
(ii) In the presence of ligand L, the trigonal bipyramid **A(L)** turns to a distorted tetrahedral **B(L)**, as shown by the angles at Cu which all come closer to 110°. The $N_{bas}–Cu–N_{bas}$ angle remains unchanged within 110–116°. The $N_{ap}–Cu–L$ angle decreases significantly from 180° to a value of (127.5 ± 1.5)° and the $N_{ap}–Cu–N_{bas}$ angles, despite the constraint by the tripod arms, increase to (83 ± 3)° (a value close to that in **A(Ø)** structures).

Table 3
Potential energies and Gibbs free energies (kcal mol^{-1}, at 213 K) and geometric data (distances in Å and angles in degrees, ⟨. . .⟩ stands for average value over all equivalent distances) for **A(L)** and **B(L)** complexes. The symbols for geometrical values are described in the text and for energetic data in the computational details part.

L	TMPA				tren			
	Ø	CO	CH_3CN	PH_3	**Ø**	CO	CH_3CN	PH_3
$\Delta E(B/A)$	9.4	3.9	4.7	2.4	12.6	3.1	3.6	3.3
$E(A)$	0.0	−15.6	−15.5	−8.1	0.0	−15.1	−15.2	−9.3
$E(B)$	9.4	−11.7	−10.8	−5.7	12.6	−12.0	−11.6	−5.9
$\Delta E_c(B)$	N.C.	−21.1	−20.2	−15.1	N.C.	−24.6	−24.2	−18.6
$\Delta G(B/A)$	8.8	3.9	3.8	2.5	11.6	2.7	2.7	2.7
$G(A)$	0.0	−8.2	−8.1	−0.3	0.0	−7.6	−8.7	−5.9
$G(B)$	8.8	−4.3	−4.3	2.2	11.6	−4.9	−6.0	1.3
$\Delta G_c(B)$	N.C.	−13.1	−13.1	−6.6	N.C.	−16.5	−17.6	−10.3
Cu–L(A)	N.C.	1.87	2.04	2.31	N.C.	1.88	2.02	2.31
Cu–L(B)	N.C.	1.83	1.92	2.23	N.C.	1.83	1.92	2.23
Cu–N_{ap}(A)	2.25	2.50	2.50	2.49	2.26	2.71	2.66	2.71
Cu–N_{ap}(B)	2.30	2.21	2.29	2.26	2.32	2.21	2.27	2.25
⟨Cu–N_{bas}(A)⟩	2.04	2.18	2.14	2.19	2.11	2.20	2.20	2.21
⟨Cu–N_{bas}(B)⟩	1.93	2.08	2.07	2.09	1.97	2.12	2.14	2.14
$\Omega(A)$	153	125	128	126	160	123	128	124
N_{bas}–Cu–N_{bas}(B)	168	111	116	113	158	110	114	111
$\Sigma(A)$	82	73	74	73	84.	72.	74.	72.
$\Sigma(B)$	84	81	80	80	86.	85.	84.	84.
N_{ap}–Cu–L(A)	N.C.	180	180	179	N.C.	180	179	180
N_{ap}–Cu–L(B)	N.C.	128	127	129	N.C.	127	126	129

The Cu–L bond lengths significantly decrease upon the decoordination of the arm, in good agreement with the energetic data which show that the energies of coordination of L in the tetracoordinated **B(L)** forms (values of $\Delta E_c(B)$ in Table 3, ranging from −15.5 to −24.6 kcal mol^{-1} depending on the nature of L and the tripod) are significantly larger than the binding energies of L in the pentacoordinated **A(L)** forms (from −8.1 to −15.6 kcal mol^{-1}, see $E(A)$ values in Table 3).

As a consequence, the decoordination energy $\Delta E(B/A)$ of one of the arms of the tripod is significantly larger in the absence of ligand L (endoenergetic by 9.4 kcal mol^{-1} for TMPA and by 12.6 kcal mol^{-1} for tren) than when ligand L is already coordinated (between +2.4 and +4.7 kcal mol^{-1}). This is associated to a different geometric behavior as the structural differences between **B(Ø)** and **B(L)** are much larger than those between **A(Ø)** and **A(L)**. As these results are similar when Gibbs free energies are concerned, it can be concluded that **B** is highly disfavored in absence of additional ligand, whereas is becomes competitive with the **A** form in presence of a ligand.

It is tempting to use these data to carry out a systematic comparison to the numerous experimental results available on these systems. However, the model considered for the tripod and the absence of counter-ion [41] and of solvent effects does not allow direct comparison. For instance, acetonitrile and carbonyl ligands are found to have similar ΔG whereas CO is experimentally found to displace CH_3CN [18]. Another example concerns PR_3 bonding complex, for which the **A** structure is found to be favored theoretically (R = H) whereas the B structure is observed from X-Ray data (R = Ph) [23]. In addition, the absence of BSSE corrections was shown in the experimental details to forbid the comparison for binding energies between two different ligands.

Let us finally give a first piece of answer to the question of the title that is, what is the result of the competition between arm and ligand binding? This is obtained from the $E(B)$ and $G(B)$ values, which correspond to the process: **A(Ø)** + **L** → **B(L)**. In the case of the prototype L = CO and CH_3CN ligands, intramolecular binding of one arm is disfavored over coordination of incoming ligands L. For the less coordinating PH_3 ligand, its binding is energetically favored over that of a nitrogenated arm, in good agreement with the HSAB rule stating that, in presence of other nitrogen ligands [42], the rather *soft* copper (I) cation preferentially binds *soft* ligands as phosphines over *hard*er ligands such amines, but the entropic cost of the intermolecular binding for PH_3 leads to a slightly positive Gibbs free energy $G(B)$.

4. Coordination of water and alcohol

A significantly different bonding scheme is obtained when examining the coordination of water and alcohol ligands ROH with R = H, methyl (Me) and phenyl (Ph) to the copper center (Table 4).

The **A(ROH)** structures could only be optimized in the case of the TMPA ligand as the model used for tren introduces an unrele-

Table 4
Potential energies and Gibbs free energies (kcal mol^{-1}, at 213 K) and geometric data (distances in Å and angles in degrees, ⟨. . .⟩ stands for average value over all equivalent distances) for **B(ROH)** and **C(ROH)** complexes. The symbols for energetic data are described in the text.

	TMPA			tren		
	H_2O	MeOH	PhOH	H_2O	MeOH	PhOH
$\Delta E_c(B)$	−7.1	−8.5	−6.8	−10.1	−11.4	−10.0
$E(A)$	−6.3	−6.7	−6.6	N.C.	N.C.	N.C.
$E(B)$	2.3	0.9	2.6	2.6	1.3	2.6
$E(C)$	−5.8	−6.5	−7.1	−7.2	−8.1	−7.8
$\Delta E(B/C)$	8.1	7.4	9.7	9.8	9.3	10.4
$\Delta G_c(B)$	−0.5	−1.5	0.0	−3.6	−4.2	−2.7
$G(A)$	0.6	0.6	0.8	N.C.	N.C.	N.C.
$G(B)$	8.3	7.3	9.1	8.0	7.4	9.0
$G(C)$	3.1	2.5	2.1	1.1	0.4	0.3
$\Delta G(B/C)$	5.2	4.8	6.9	7.0	7.1	8.7
Cu–N_{ap}(A)	2.32	2.33	2.32	N.C.	N.C.	N.C.
Cu–N_{ap}(B)	2.33	2.31	2.30	2.31	2.30	2.33
Cu–N_{ap}(C)	2.35	2.35	2.35	2.38	2.38	2.38
⟨Cu–N_{bas}(A)⟩	2.06	2.06	2.06	N.C.	N.C.	N.C.
⟨Cu–N_{bas}(B)⟩	2.00	2.01	2.01	2.05	2.06	2.04
⟨Cu–N_{bas}(C)⟩	2.01	2.02	2.01	2.07	2.08	2.06
Cu–O(A)	2.82	2.73	2.73	N.C.	N.C.	N.C.
Cu–O(B)	2.20	2.15	2.17	2.26	2.20	2.30
Cu–O(C)	2.11	2.09	2.13	2.10	2.08	2.10
N. . .H(C)	1.72	1.75	1.71	1.73	1.76	1.71
O–H(B)	0.97	0.97	0.97	0.97	0.97	0.97
O–H(C)	1.00	1.00	1.01	1.01	1.00	1.01
N_{ap}–Cu–O(A)	164	166	172	N.C.	N.C.	N.C.
N_{ap}–Cu–O(B)	126	118	119	118	118	124
N_{ap}–Cu–O(C)	107	108	107	106	108	107
N_{bas}–Cu–N_{bas}(A)	117	117	117	N.C.	N.C.	N.C.
N_{bas}–Cu–N_{bas}(B)	135	131	130	139	134	140
N_{bas}–Cu–N_{bas}(C)	128	127	131	129	128	131

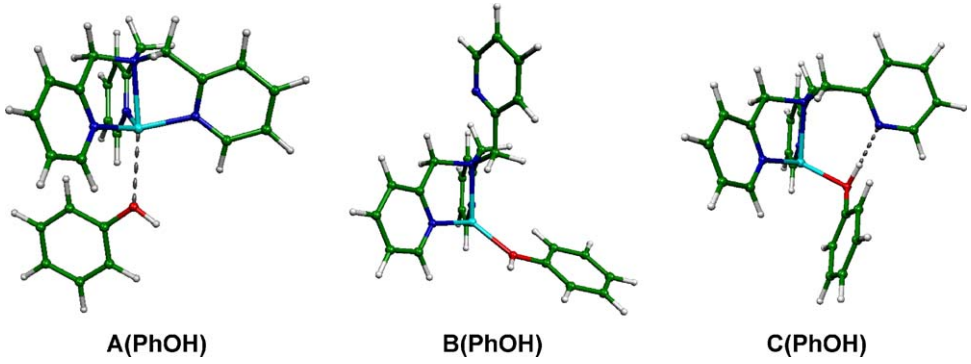

Fig. 2. Coordination of phenol (PhOH) to the $[Cu(TMPA)]^+$ complex in the vacant site (left structure, **A(PhOH)**), with a dangling arm (center, structure **B(PhOH)**) and with an H-bonded arm (right, structure **C(PhOH)**).

vant parasitic hydrogen bond between the hydrogen of the model NH_2 group located at the end of the tripod's arms and the oxygen hydroxyl function of the incoming ligand (NH_2...OH interactions). For TMPA, the **A(ROH)** structures are found to exhibit small binding energies close to −6.5 kcal mol^{-1}, leading to Gibbs free energies close to zero. In good agreement, the Cu...O distances are long (between 2.73 and 2.82 Å) whereas the geometric features characteristic of the tripod are almost unaltered with respect to the **A(Ø)** structure. The ROH ligand in the **A(ROH)** structures can thus be considered as quasi-unbounded.

Stronger interactions of the alcohol ligand to the metal center are obtained when decoordination of one of the tripod arms takes place. As illustrated in Fig. 2 in the case of the phenol ligand, two types of structures are obtained which implies either a full decoordination of one arm – structure **B(ROH)** – or the insertion of ligand ROH within one of the Cu–N_{bas} bond to result in the formation of an hydrogen bond between the nitrogen of the arm and the OH group of the ligand – structure **C(ROH)**.

The structures **B(ROH)** are closely related to those observed for the prototype ligands (Table 4): the N_{ap}–Cu–O(H)R angle lies between 118 and 126° which is close to the 127° value obtained on average for the **B(L)** structures (L = CO, CH_3CN or PH3). The N_{bas}–Cu–N_{bas} angle lies between 130 and 140°, which is significantly larger than the 113° value obtained in average for the prototype ligands, but remain much smaller than the 163° value obtained in average for structures **B(Ø)**. The binding energy of water or alcohols to the copper center ($\Delta E_c(B)$ in Table 4) in structures **B(ROH)** amounts to about 7.1 and 10.4 kcal mol^{-1}, which is significantly smaller than the values obtained for **B(CO), B(CH_3CN)** and even **B(PH_3)** (all larger than 15 kcal mol^{-1}, see Table 3). Finally, a constant trend concerning the effect of the tripod can observed for forms **B** whatever the ligand: the coordination to the tren containing complexes is larger than the coordination to the TMPA containing systems.

Most surprisingly, despite the fact that they are formally obtained by insertion of ligand ROH within the Cu...O bond in **A(Ø)** structures (see below for mechanistic insight), structures **C(ROH)** are very close to **B(ROH)** and are even closer to an ideal tetrahedron. This is evidenced by the N_{ap}–Cu–O(H)R and the N_{bas}–Cu–N_{bas} angles which are closer to 109° in structures **C** than in the corresponding **B** forms. In particular, this corresponds to a diminution of the N_{ap}–Cu–O angles, which can be associated to an attraction of the alcohol ligand by the arm through the H bond. The energy of the H-bond can be evaluated as the energy difference between structures **C(ROH)** and **B(ROH)** and is reported in Table 4 in entry "$\Delta E(B/C)$". It lies between 7.4 and 10.4 kcal mol^{-1}, depending on the nature of R and of the tripod. A rational of the strength of the hydrogen bond is easily obtained using the acidity constant of the alcohols: the more acidic the alcohol (PhOH > H_2O > MeOH), the stronger the H-bond (the larger the $\Delta E(B/C)$ values). Similarly, the less basic pyridine (pK_a = 5.3) makes weaker bonds than the more basic primary amine (pK_a = 10.7 for ethanamine). The H-bond distance is found to be only marginally dependent on the nature of R but follows a similar trend: the larger the binding energy, the smaller the N...H distance. The OH bonds are hardly altered by the H-bond and are not significantly affected by the nature of R.

The energies of structures **C** thus result from the competition between three phenomena, according to the decomposition steps proposed in Scheme 3:

(i) The decoordination of an arm of the tripod quantified by $\Delta E(B/A)$ in Table 3 for structures **B(Ø)**. It is found to be easier for TMPA than for tren.
(ii) The coordination of the alcohol, given by $\Delta E_c(B)$ in Table 4, which is found to be larger for tren than for TMPA, but also slightly smaller than the arm decoordination (contribution *i*) so that $E(B)$ energies for structures **B(ROH)** are slightly positive.
(iii) The formation of a strong hydrogen bond, given by $\Delta E_{B/C}$ in Table 4, which allows structures **C(ROH)** to be lower in energy than the separated **A(Ø)** and ROH. When entropic effects are included, the formation of **C(ROH)** from the separated starting material is thus quasi-neutral, as observed from the very small Gibbs free energy values, and slightly more favored in the case of the tren containing complexes.

We next examine whether it is necessary to undergo full decoordination of the tripod arm to allow formation of structure **C(ROH).** This study was carried out in the case of the TMPA tripod and insertion of water was examined. The results are given in Fig. 3. A transition state (TS) for insertion of water within the Cu–N bond is found only 6.0 kcal mol^{-1} above **A(H_2O)** in Gibbs free energy. This reaction is thus found to be an easy transformation, as the Cu...N bond breaking is only partial in the TS (from 2.06 Å in **A(H_2O)** to 2.76 Å in the TS compared to 3.56 Å in **C(H_2O)**) whereas the Cu...O bond is strongly reinforced when going from the starting material (2.85 Å) to the TS (2.25 Å) whereas a very small shortening is observed to reach the product (2.11 Å).

In comparison, all dissociative pathways have to go through **B(ROH)** geometries, which is always more than 7.6 kcal mol^{-1} above **A(ROH)** and is thus not a competitive possible reaction.

5. Dioxygen adducts

In this final Section, we investigate the coordination of dioxygen to the $[Cu(N_3N)]^+$ moieties (Table 5 and Fig. 4). We here only consider *end-on* coordination in the triplet spin state since it has been suggested to be the most energetically favorable coordination mode in the case of N_3N ligands [9]. Dioxygen binding energy

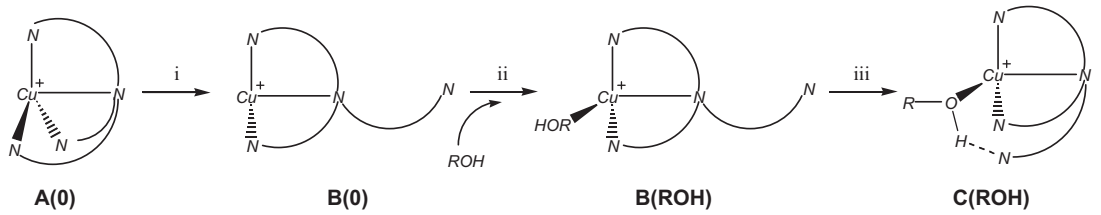

Scheme 3.

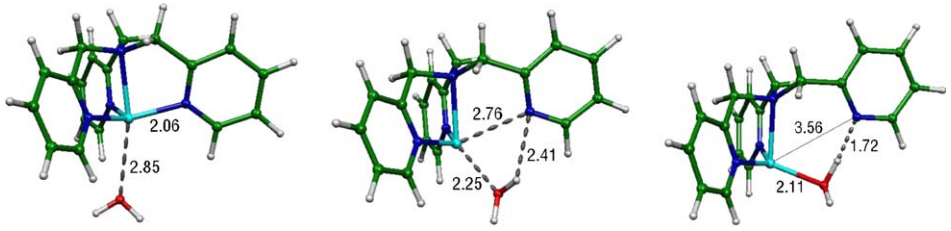

Fig. 3. Structures (distances in Å), potential energies/Gibbs free energies (with respect to dissociated **A(Ø)** and water in kcal mol^{-1}) for the reaction path for insertion of water in the Cu–N bond.

Table 5
Potential energies and Gibbs free energies (kcal mol^{-1}, at 213 K) and characteristic distances for O_2 coordination (in Å, O_p stands for the proximal oxygen) for **A(O_2)**, **B(O_2)** (values given after the/sign) and **D(ROH)** complexes. The symbols for energetic data are given in the computational details part. ΔE_{O_2} stands for the binding energy for the dioxygen ligand.

L=	TMPA				tren			
	A(O_2)/B(O_2)	D(H_2O)	D(MeOH)	D(PhOH)	**A(O_2)/B(O_2)**	D(H_2O)	D(MeOH)	D(PhOH)
$E(X)$	−9.4/3.8	−10.2	−11.1	−9.8	−7.6/6.7	−11.7	−12.7	−11.0
ΔE_{O_2}	−9.4/−5.6	−4.4	−4.6	−2.7	−7.6/−5.9	−4.5	−4.6	−3.2
$G(X)$	−1.7/10.3	5.5	5.0	5.9	−0.3/12.2	3.4	2.5	2.3
ΔG_{O_2}	−1.7/1.5	2.4	2.5	3.8	−0.3/0.6	2.3	2.1	2.1
Cu–O_p	1.99/2.05	2.07	2.07	2.09	2.01/1.99	2.09	2.08	2.12
O–O	1.27/1.27	1.26	1.26	1.26	1.27/1.27	1.26	1.26	1.26

to [Cu(TMPA)]$^+$ in the triplet state is found to be exothermic by 9.4 kcal mol^{-1}, which is slightly larger than for the coordination of PH_3 or phenol ligands. In contrast, a 7.6 kcal mol^{-1} value is obtained in the case of the tren containing complex, a value smaller than for the coordination of PH_3 or phenol. This can be understood by considering dioxygen as an acceptor-only ligand, in opposition to the mostly donor ligands PH_3 or phenol. A NPA analysis of the charges on the O_2 moiety taken in complex **A(O_2)** confirms that the larger binding energy of dioxygen in the case of the TMPA tripod correlates with a larger charge transfer to dioxygen: the charge at O_2 in the case of TMPA amounts to −0.25 electron whereas it is only −0.18 electron for tren. In addition, no decoordination of the apical nitrogen of the TMPA or tren tripod is observed upon coordination of O_2 (Cu–N_{ap} = 2.22 Å in [Cu(TMPA)(O_2)]$^+$ instead of 2.25 Å

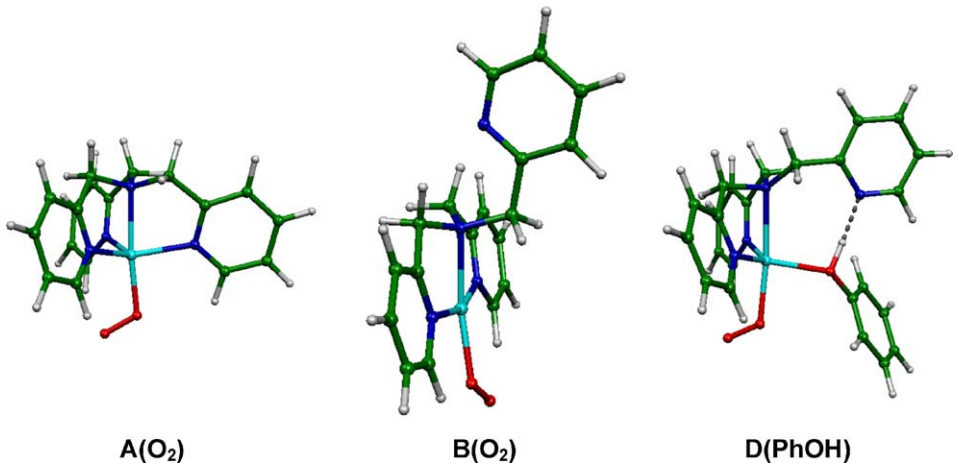

Fig. 4. Coordination of dioxygen (triplet form) to the [Cu(TMPA)]$^+$ complex in the vacant site (left structure, A(O_2)), with a dangling arm (center, structure B(O_2)) and with a phenol ligand already present (right, structure D(PhOH)).

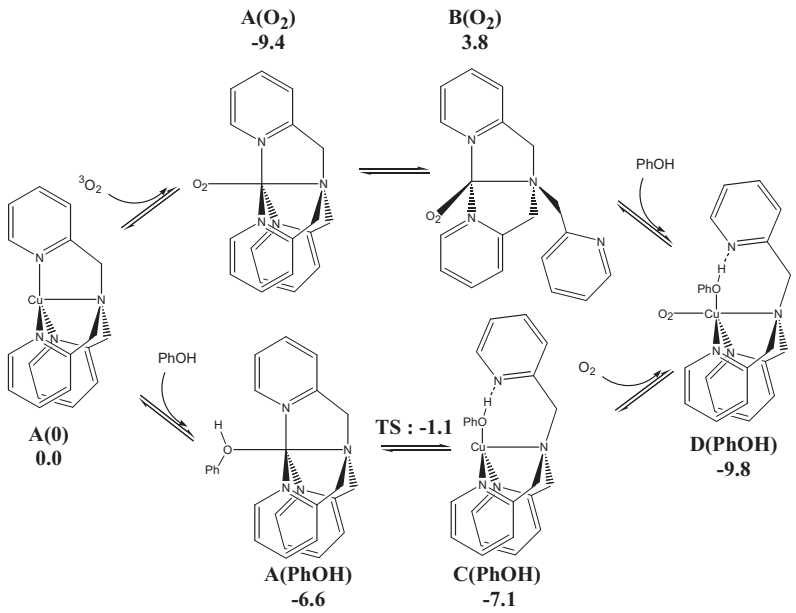

Scheme 4. Energetic (potential energy in kcal mol^{-1}) features for the possible intermediates toward the coordination of the two incoming ligands.

in [Cu(TMPA)]$^+$ and Cu–N_{ap} = 2.23 Å in [Cu(tren)(O_2)]$^+$ instead of 2.26 Å in [Cu(tren)]$^+$). The role of the apical atom in enhancing the stabilization of the [Cu(O_2)] adducts for N_3X chelating ligands has been stressed elsewhere [9].

As suggested by this bonding scheme, decoordination of one of the arms of the tripod (leading to structure **B(O_2)**, Fig. 4) is much more disfavored in the case of L = O_2 (13.2 kcal mol^{-1} in the case of TMPA and 14.3 kcal mol^{-1} for tren) than when one of the prototype ligand is present (3.5 kcal mol^{-1} in average for CO, CH_3CN and PH_3 in TMPA and tren containing tripods, see Table 3), or for the H-bonded ligands ROH (+9.1 kcal mol^{-1} in average for R = H, Me or Ph and for tren and TMPA, see Table 4), or even for the naked tripod (11.0 kcal mol^{-1} in average for TMPA and tren, see Table 3). Most surprisingly, this weaker binding is associated to a significant lengthening of the Cu–O_p distance only in the case of the TMPA tripode (from 1.99 Å to 2.05 Å), highlighting the weakening of the interaction between dioxygen and copper in this complex (which diminishes by 3.8 kcal mol^{-1}). No such lengthening is obtained for tren, in accordance with a smaller decrease of the O_2 binding energy upon decoordination of the arm (only 1.7 kcal mol^{-1}). As a consequence, the binding energy of O_2 to structure **B(Ø)** is −5.6 kcal mol^{-1} for TMPA and −5.9 kcal mol^{-1} for tren. This is significantly smaller than for the coordination of dioxygen in form **A**, in contrast to what was observed for all other ligands for which decoordination of one arm increases the binding energy of the new ligand. Decoordination of one of the tripod arms decreases dioxygen bonding, whereas it increases CO bonding.

With such a bonding scheme, it is expected that similar results should be obtained for the coordination of dioxygen to the three ROH bonded complexes **C(ROH)**. The obtained structure is referred as **D(ROH)** (Fig. 4) and results are gathered in Table 5. The binding energy of O_2 can then be computed as the difference between *E*(**D**) (Table 4) and *E*(**C**) (Table 5) for a given ROH and a given tripod. Exothermic O_2 binding is found, with values between 2.4 and 4.6 kcal mol^{-1} for the binding energy, the smallest value being found for PhOH in the tren or TMPA complex. These values are significantly smaller than in the absence of alcohol (complexes **A(O_2)**): this is in line with a less donating character of the alcohol ligands with respect to the nitrogen containing ligands, and thus with a smaller donating power of entities **C(ROH)** with respect to **A(Ø)**. In addition, long Cu...O_2 distances are found, in line with weak dioxygen binding.

6. Conclusion

We have shown that decoordination of one of the tripod arms plays a major role for the formation of reactive intermediates for the oxidation of exogenous substrates catalyzed by copper-dioxygen adducts. Indeed, such a decoordination increases the ligand binding energy for any donor ligand whereas it decreases the binding abilities of dioxygen. As a consequence, decoordination of one arm of the N_3N tripod in [Cu(N_3N)(O_2)]$^+$ (**A(O_2)**) to allow coordination of a potentially oxidized exogenous ligand (Scheme 4, top) leads to an endothermic intermediate and is thus highly unlikely. These observations lead us to propose that catalyzed oxidation of the phenolic ligand by complexes [Cu(N_3N)(O_2)]$^+$ should rather take place according to the sequence described in the bottom of Scheme 4: first, coordination of the phenolic ligand takes place in the vacant site and easy insertion within the Cu–N bond takes place leading to an H-bonded complex. With such a process, one coordination site is kept for the second incoming ligand, namely O_2. In these conditions, the whole reaction sequence is found to occur *via* low energy structures, and appears to be largely favored. In this reaction path, the formation of an H-bond between the tripod and the substrate is found to play a major role, as it allows the correct positioning of the substrate within the coordination sphere of the copper, without loss of a binding lacuna and no high energy intermediate.

This proposal for an associative reaction pathway for the reaction shown in Scheme 1 is in strong contrast with recently published results and thus deserves further examination, for example by including solvent effects. In particular, decoordination of one arm allows oxidation of the phenolic species to take place in a monomolecular mechanism, which prevents the strong entropic costs associated to bimolecular steps. The full reaction path is currently under study.

References

[1] P.T. Anastas, J.C. Warner, Green Chemistry: Theory and Practice, Oxford University Press, New York, 1998.
[2] B.M. Trost, Science 254 (1991) 1471.

[3] L. Que Jr., W.B. Tolman, Nature 455 (2008) 333–340.
[4] E.A. Lewis, W.B. Tolman, Chem. Rev. 104 (2004) 1047–1076.
[5] S. Itoh, Curr. Opin. Chem. Biol. 10 (2006) 115–122.
[6] S. Fukuzumi, H. Kotani, H.R. Lucas, K. Doi, T. Suenobu, R.L. Peterson, K.D. Karlin, J. Am. Chem. Soc. 132 (2010) 6874–6875.
[7] J.P. Piquemal, J. Maddaluno, B. Silvi, C. Giessner-Prettre, New J. Chem. 27 (2003) 909.
[8] J.P. Piquemal, J. Pilme, Mol. Struct. Theochem. 764 (2006) 77.
[9] A. de la Lande, H. Gérard, V. Moliner, G. Izzet, O. Reinaud, O. Parisel, J. Biol. Inorg. Chem. 11 (2006) 593.
[10] A. de la Lande, V. Moliner, O. Parisel, J. Chem. Phys. 126 (2007) 035102.
[11] A. de la Lande, H. Gérard, O. Parisel, Int. J. Quant. Chem. 108 (2008) 1898–1904.
[12] A. de la Lande, O. Parisel, H. Gérard, V. Moliner, O. Reinaud, Chem. Eur. J. 14 (2008) 6465–6473.
[13] A. de la Lande, D.R. Salahub, V. Moliner, H. Gérard, J.-P. Piquemal, O. Parisel, Inorg. Chem. 48 (2009) 7003–7005.
[14] A. de la Lande, D.R. Salahub, J. Maddaluno, A. Scemama, J. Pilmé, O. Parisel, H. Gérard, M. Caffarel, J.-P. Piquemal, J. Comput. Chem. 32 (2011) 1178–1182.
[15] G. Izzet, J. Zeitouny, H. Akdas-Killig, Y. Frapart, S. Ménage, B. Douziech, I. Jabin, Y. Le Mest, O. Reinaud, J. Am. Chem. Soc. 130 (2008) 9514–9523.
[16] N. Le Poul, B. Douziech, J. Zeitouny, G. Thiabaud, H. Colas, F. Conan, N. Cosquer, I. Jabin, C. Lagrost, P. Hapiot, O. Reinaud, Y. Le Mest, J. Am. Chem. Soc. 131 (2009) 17800–17807.
[17] K.D. Karlin, S. Fox, A. Nanthakumar, N.N. Muthy, W. Wei, H.V. Obias, C.F. Martens, Pure Appl. Chem. 67 (1995) 289–296.
[18] C.X. Zhang, S. Kaderli, M. Costas, E.-I. Lim, Y.-M. Neuhold, K.D. Karlin, A.D. Zuberbühler, Inorg. Chem. 442 (2003) 1807.
[19] L.M. Mirica, X. Ottenwaelder, T.D.P. Stack, Chem. Rev. 104 (2004) 1013–1045.
[20] D. Maiti, H.C. Fry, J.S. Woertink, M.A. Vance, E.I. Solomon, K.D. Karlin, J. Am. Chem. Soc. 129 (2007) 264–265.
[21] D. Maiti, D.-H. Lee, K. Gaoutchenova, C. Würtele, M.C. Holthausen, A.A. Narducci Sarjeant, J. Sundermeyer, S. Schindler, K.D. Karlin, Angew. Chem. Int. Ed. 47 (2008) 82–85.
[22] M. Güell, J.M. Luis, P.E.M. Siegbahn, M. Sola, J. Biol. Inorg. Chem. 14 (2009) 273–285.
[23] Z. Tyeklár, R.R. Jacobson, N. Wei, N.N. Murthy, J. Zubieta, K.D. Karlin, J. Am. Chem. Soc. 155 (1993) 2677–2689.
[24] D.-H. Lee, L. Wei, N.N. Murthy, Z. Tyeklár, K.D. Karlin, S. Kaderli, B. Jung, A.D. Zuberblither, J. Am. Chem. Soc. 177 (1995) 12498.
[25] H.R. Lucas, G.J. Meyer, K.D. Karlin, J. Am. Chem. Soc. 132 (2010) 12927–12940.
[26] M.J. Frisch, G.W. Trucks, H.B. Schlegel, G.E. Scuseria, M.A. Robb, J.R. Cheeseman, J.A. Montgomery Jr., T. Vreven, K.N. Kudin, J.C. Burant, J.M. Millam, S.S. Iyengar, J. Tomasi, V. Barone, B. Mennucci, M. Cossi, G. Scalmani, N. Rega, G.A. Petersson, H. Nakatsuji, M. Hada, M. Ehara, K. Toyota, R. Fukuda, J. Hasegawa, M. Ishida, T. Nakajima, Y. Honda, O. Kitao, H. Nakai, M. Klene, X. Li, J.E. Knox, H.P. Hratchian, J.B. Cross, V. Bakken, C. Adamo, J. Jaramillo, R. Gomperts, R.E. Stratmann, O. Yazyev, A.J. Austin, R. Cammi, C. Pomelli, J.W. Ochterski, P.Y. Ayala, K. Morokuma, G.A. Voth, P. Salvador, J.J. Dannenberg, V.G. Zakrzewski, S. Dapprich, A.D. Daniels, M.C. Strain, O. Farkas, D.K. Malick, A.D. Rabuck, K. Raghavachari, J.B. Foresman, J.V. Ortiz, Q. Cui, A.G. Baboul, S. Clifford, J. Cioslowski, B.B. Stefanov, G. Liu, A. Liashenko, P. Piskorz, I. Komaromi, R.L. Martin, D.J. Fox, T. Keith, M.A. Al-Laham, C.Y. Peng, A. Nanayakkara, M. Challacombe, P.M.W. Gill, B. Johnson, W. Chen, M.W. Wong, C. Gonzalez, J.A. Pople, Gaussian 03, Revision C.02, Gaussian Inc., Wallingford, CT, 2004.
[27] N. Godbout, D.R. Salahub, J. Andzelm, E. Wimmer, Can. J. Chem. 70 (1992) 560.
[28] R. Krishnam, J.S. Binkley, R. Seeger, J.A. Pople, J. Chem. Phys. 72 (1980) 650.
[29] P.M.W. Gill, B.G. Johnson, J.A. Pople, M. Frisch, J. Chem. Phys. Lett. 197 (1992) 499.
[30] A.D. Becke, Phys. Rev. A 38 (1988) 3098.
[31] C. Lee, W. Yang, R.G. Parr, Phys. Rev. B 37 (1988) 785.
[32] B. Miehlich, A. Savin, H. Stoll, H. Preuss, Chem. Phys. Lett. 157 (1989) 200.
[33] A.D. Becke, J. Phys. Chem. 98 (1993) 5648.
[34] J.-M. Ducéré, A. Goursot, D. Berthomieu, J. Phys. Chem. A 109 (2005) 400.
[35] J.-P. Piquemal, A. Marquez, O. Parisel, C. Giessner-Prettre, J. Comput. Chem. 26 (2005) 1052.
[36] M.P. Anderson, P. Uvdal, J. Phys. Chem. A 109 (2005) 2937–2941.
[37] S. Simon, M. Duran, J.J. Dannenberg, J. Chem. Phys. 105 (1996) 11024.
[38] S.F. Boys, F. Bernardi, Mol. Phys. 19 (1970) 553.
[39] M. Cossi, G. Scalmani, N. Rega, V. Barone, J. Chem. Phys. 117 (2002) 43, and references therein.
[40] NBO Version 3.1, E.D. Glendening, Q.E. Reed, J.E. Carpenter, F. Weinhold, To be complemented by A.E. Reed, L.A. Curtiss, F. Weinhold, Chem. Rev. 88 (1988) 899, and references therein.
[41] G.J. Christian, A. Llobet, F. Maseras, Organometallics 23 (2004) 5530–5539.
[42] C. Sivasankar, N. Sadhukhan, J.K. Bera, A.G. Samuelson, New J. Chem. 31 (2007) 385–393.